

## Supporting Information

### **Amnion-on-a-chip: modeling human amniotic development in mid-gestation from pluripotent stem cells**

Yujuan Zhu,<sup>a,d,f</sup> Hui Wang,<sup>a,d,f</sup> Fangchao Yin,<sup>a,d</sup> Yaqiong Guo,<sup>a,d</sup> Fei Li<sup>e</sup>, Dong Gao,<sup>e</sup> and Jianhua

Qin<sup>\*a,b,c,d</sup>

<sup>a</sup> CAS Key Laboratory of Separation Science for Analytical Chemistry, Dalian Institute of Chemical Physics, Chinese Academy of Sciences.

<sup>b</sup> Institute for Stem Cell and Regeneration, Chinese Academy of Sciences, Beijing, China  
Academy of Sciences, Shanghai, China

<sup>c</sup> CAS Center for Excellence in Brain Science and Intelligence Technology, Chinese Academy of Sciences, Shanghai, China

<sup>d</sup> University of Chinese Academy of Sciences, Beijing, China

<sup>e</sup> Shanghai Institute of Biochemistry and Cell Biology, Shanghai, China

<sup>f</sup> Y. Zhu and H. Wang contributed equally to this work.

Corresponding author: Prof. J. Qin, E-mail: [jqin@dicp.ac.cn](mailto:jqin@dicp.ac.cn)

## Figures

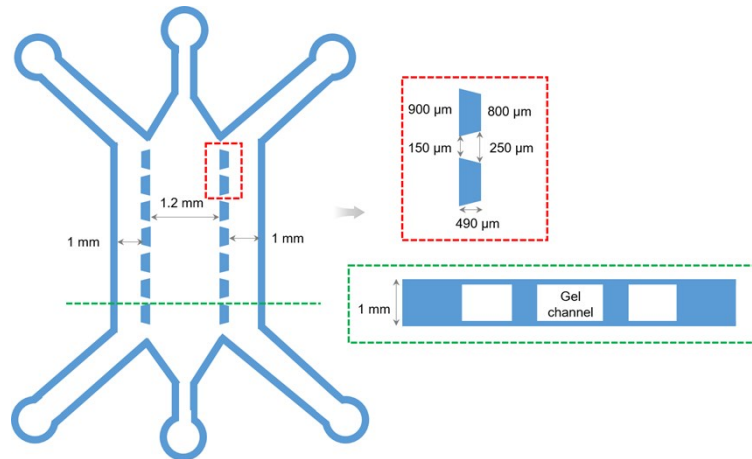


Figure S1, Schematic of the microfluidic chip design. The chip was fabricated with multichannels, including two parallel microchannels (height, 1 mm; width, 1 mm) separated by a gel microchannel (height, 1 mm; width, 1.2 mm) in the middle. The dimensions of micropillar and cross-section are indicated on the right.

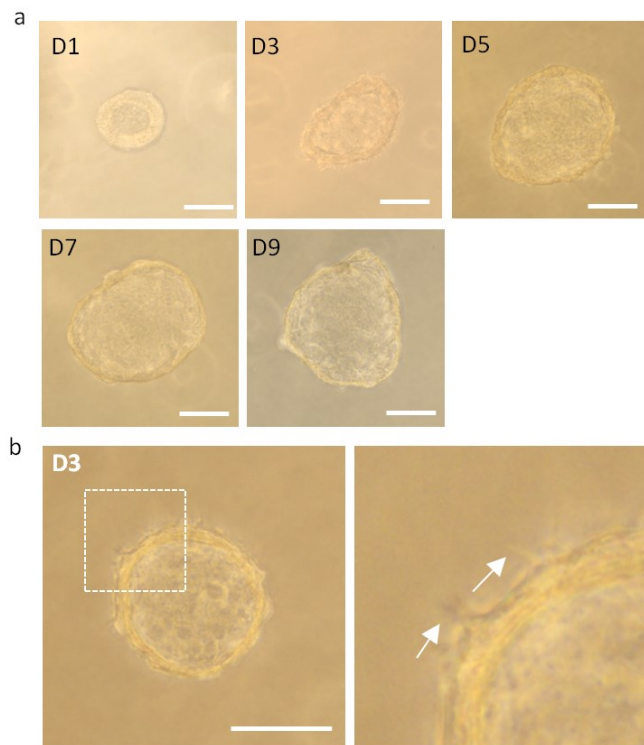
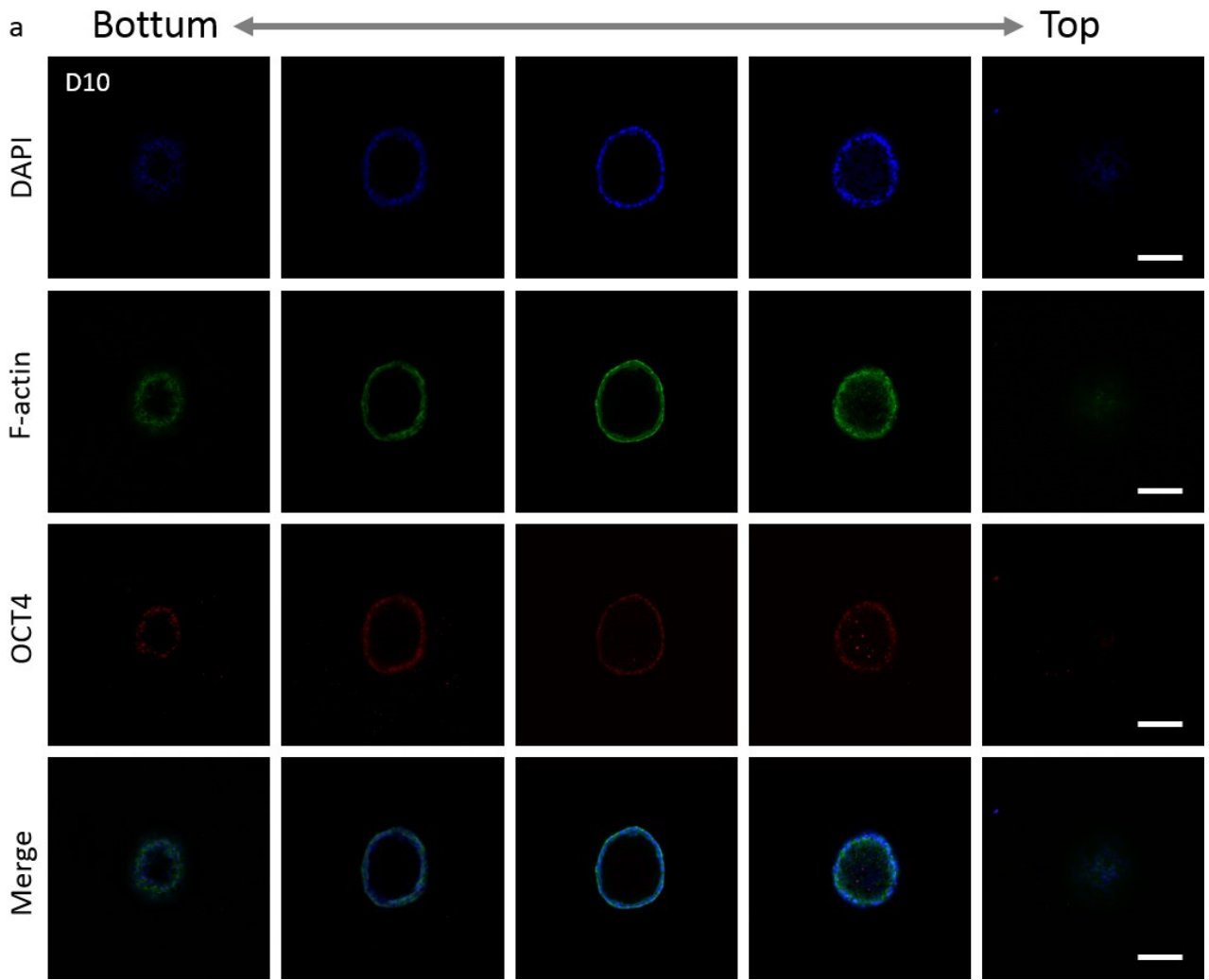


Figure S2, a, Real-time tracing of a single cell cavity in the same field of view from day 1 to 9. b, Bright-field images of epithelial protrusions from hPSC cavity. The white square highlights epithelial protrusions (white arrows). Scale bar, 100  $\mu\text{m}$ .



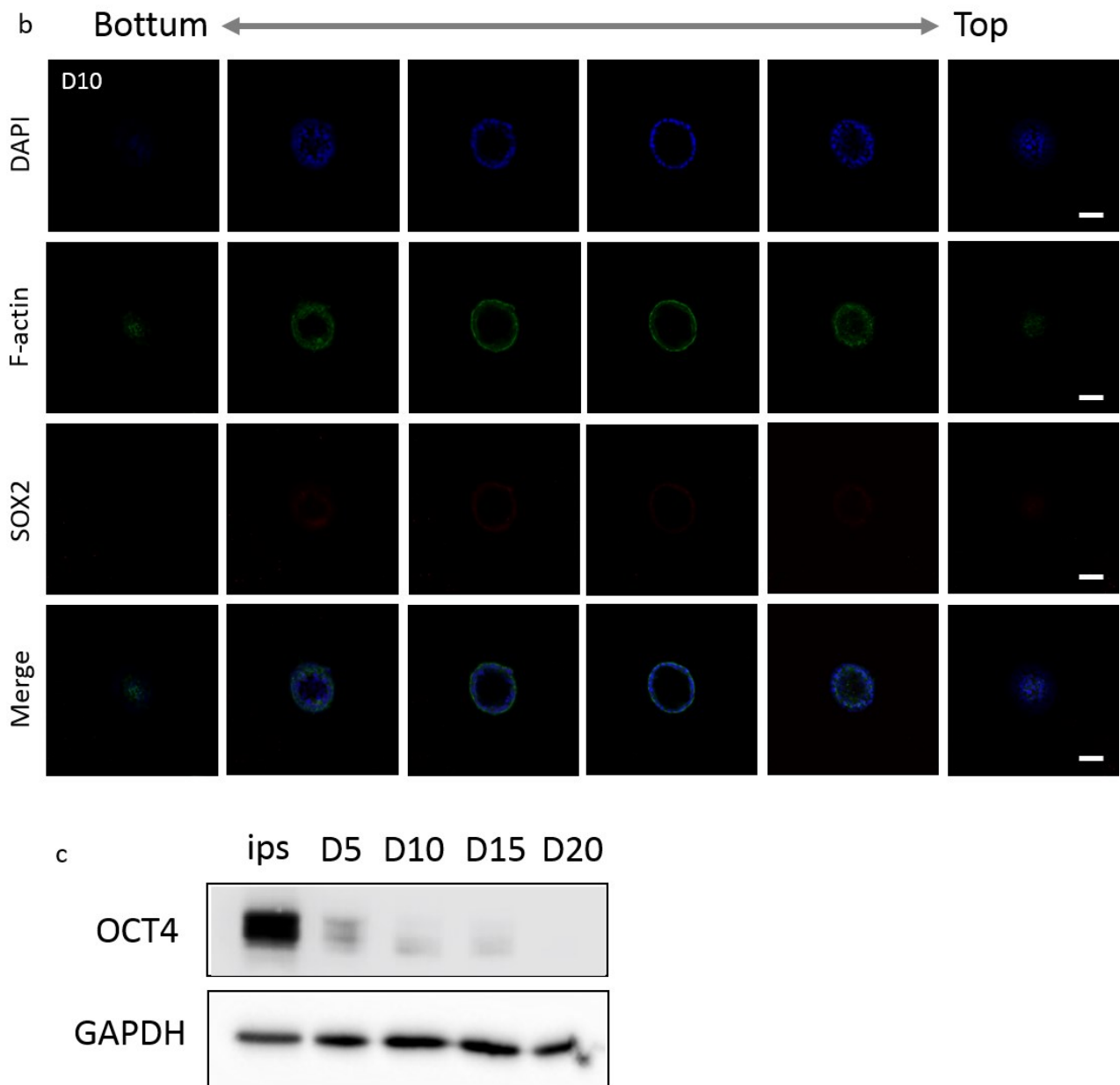


Figure S3, The expression of pluripotency markers during the formation of squamous cavity. a-b, Fluorescent staining for pluripotent markers OCT4 (a) and SOX2 (b). A series of images stained were obtained from the bottom to the top of cell cavity. Scale bar, 100  $\mu$ m (a). 50  $\mu$ m (b). c, Western Blot analysis of pluripotent marker OCT4 in cell cavity at different days.

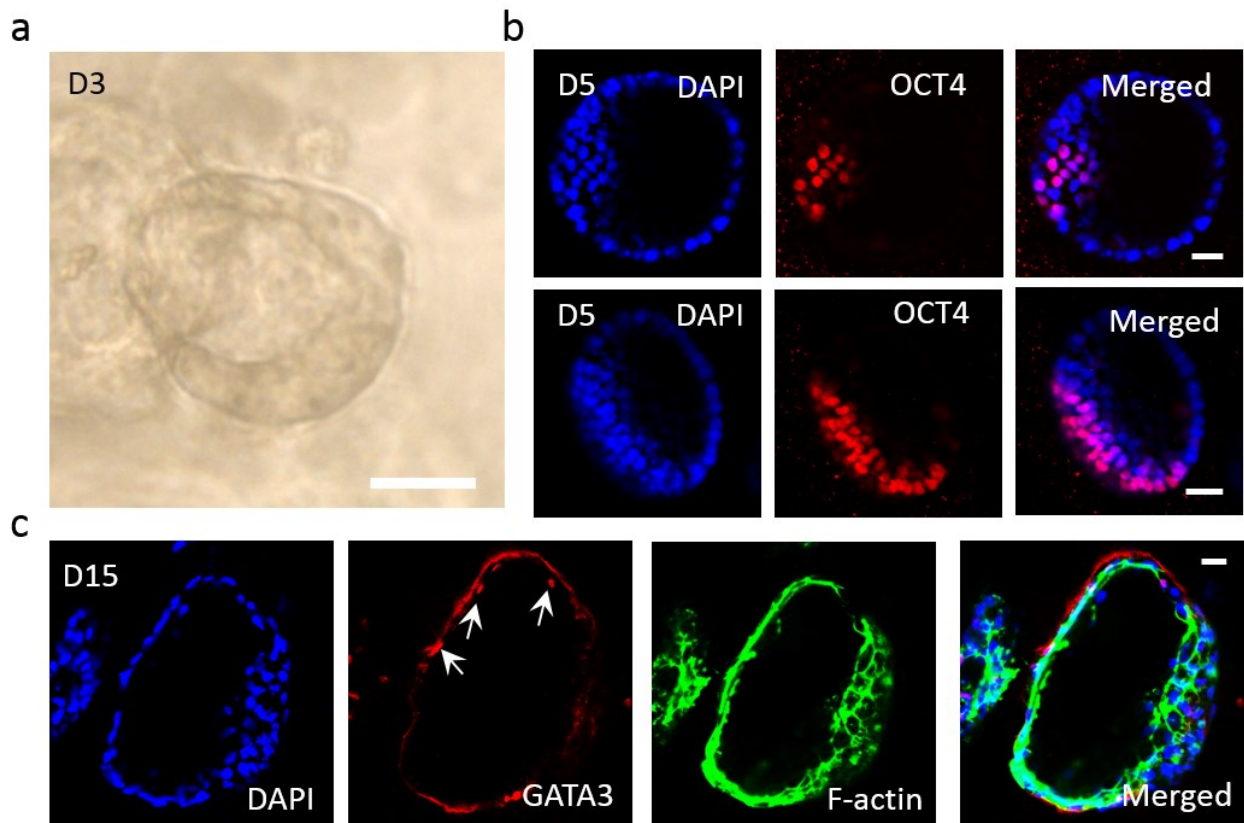


Figure S4. Characteristic of asymmetric amniotic sac-like tissue. **a**, Representative right-field image showing a asymmetric cyst with a squamous and columnar pole. **b**, Immunostaining for OCT4 in cell cavities at 5 days of differentiation. **c**, Staining for GATA3 and F-actin in cell cavities at 15 days of differentiation. White arrows indicate GATA3-positive cells at the squamous pole. Scale bars, 25  $\mu\text{m}$ .

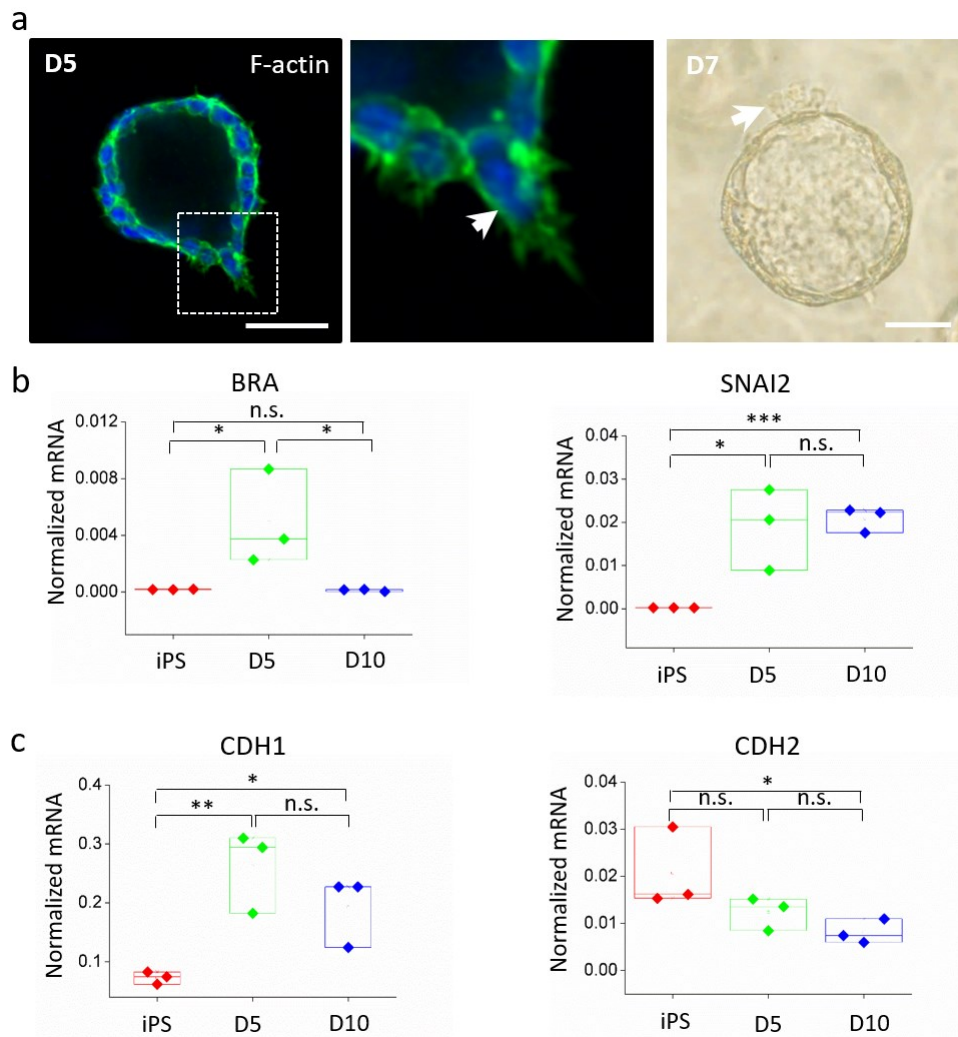


Figure S5. Invasive behavior in amnion-like cavities. **a**, Confocal micrographs and bright field images showing cell invasion from cell cavity. White arrows indicated cell migrated from cell cavities. F-actin (green) was stained. Scale bars, 50  $\mu\text{m}$ . **b-c**, qRT-PCR analysis of BRA, SNAI2, CDH1 and CDH2 for hPSC (control) and cell cavities at 5 and 10 days of differentiation. mRNA expression was normalized against a GAPDH control and data were plotted as the mean  $\pm$  SD, with three biological triplicates. \*  $P < 0.05$ . \*\*  $P < 0.01$ , \*\*\*  $P < 0.001$ , n.s., not significant.

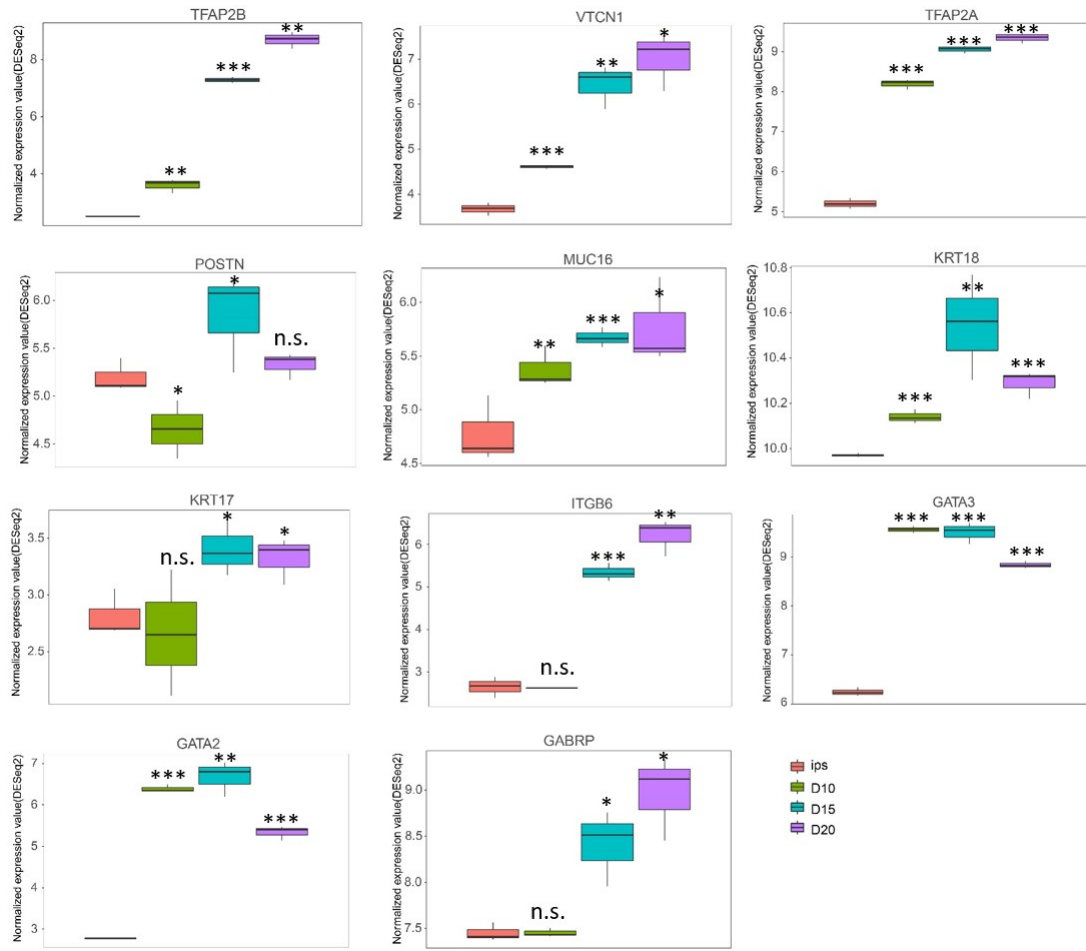
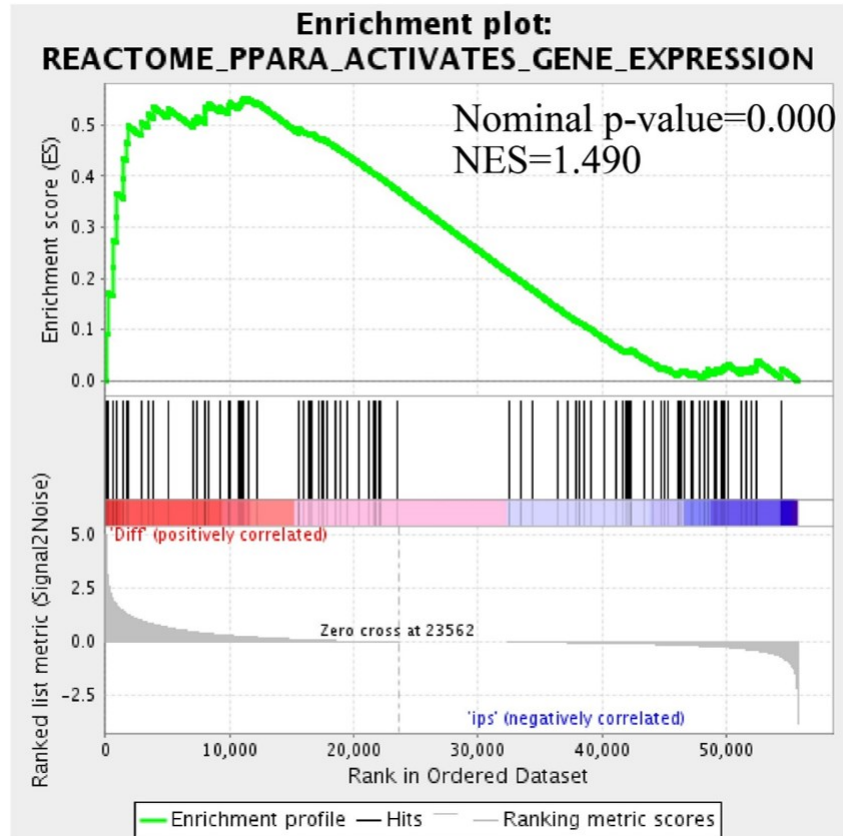
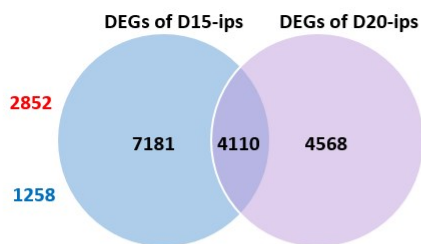


Figure S6. RNA-seq displayed mRNA expression of amnion-specific genes in hPSC, D10, D15 and D20 hPSC-amnion. \*  $P < 0.05$ . \*\*  $P < 0.01$ , \*\*\*  $P < 0.001$ , n.s., not significant.

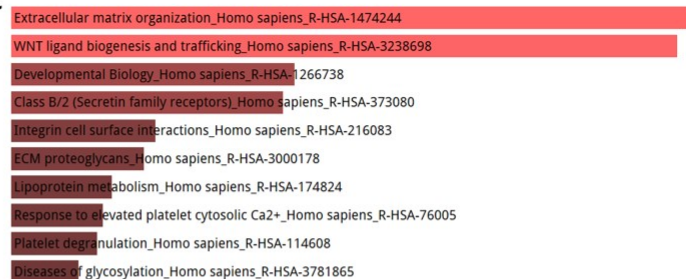
a



b



c



d

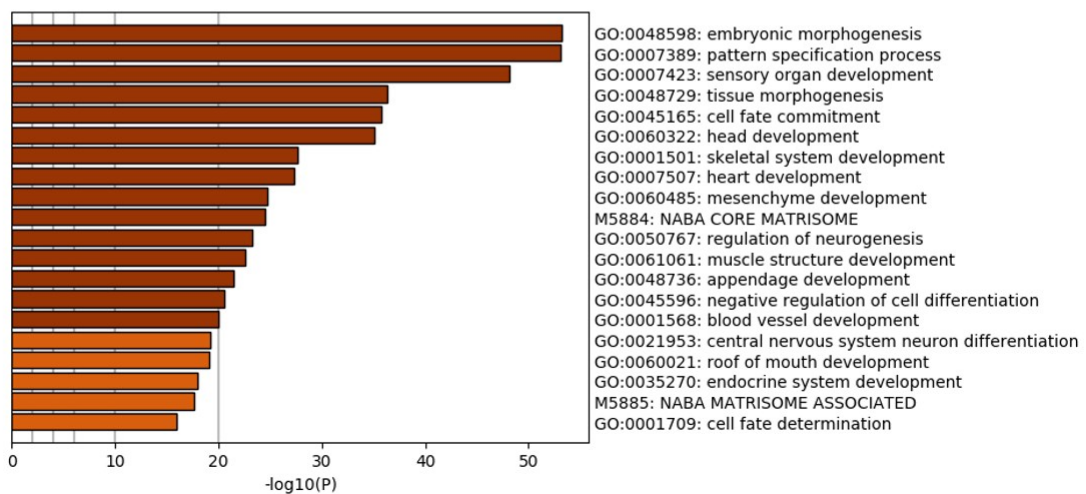


Figure S7. a, Upregulated gene set-PPARA activates gene expression in hPSC-amnion comparing with hPSC. b, A pie chart showing the significantly altered genes in D15 and D20 hPSC-amnion compared to hPSC. In total, 7181 DEGs were detected in D15 hPSC-amnion and 4568 DEGs D20

hPSC-amnion. 4110 DEGs were overlapped in both D15 and D15 hPSC-amnion, including 2852 upregulated genes and 1258 downregulated genes. c, Enriched pathway analysis of 4110 DEGs with Enrichr. e, Gene ontology (GO) functional classification of 4110 DEGs.

Table S1. A list of primer pairs for qRT-PCR.

Primer name	Sequence
OCT4A	Fw 5'-GGA GAA GCT GGA GCA AAA CC-3' Rv 5'-TGG CTG AAT ACC TTC CCA AA-3'
NANOG	Fw 5'-GAT TTG TGG GCC TGA AGA AA-3' Rv 5'-CTT TGG GAC TGG TGG AAG AA-3'
CDH2	Fw 5'- ATC AAC CCC ATA CAC CAG CC-3' Rv 5'- GTC GAT TGG TTT GAC CAC GG-3'
VTCN1	Fw 5'- TCT GGG CAT CCC AAG TTG AC-3' Rv 5'- TCC GCC TTT TGA TCT CCG ATT-3'
GABRP	Fw 5'- TTT CTC AGG CCC AAT TTT GGT-3' Rv 5'- GCT GTC GGA GGT ATA TGG TGG-3'
MUC16	Fw 5'- GGA GCA CAC GCT AGT TCA GAA-3' Rv 5'- GGT CTC TAT TGA GGG GAA GGT-3'
HAND1	Fw 5'- CCA AGG ATG CAC AGT CTG G-3' Rv 5'- AGG AGG AAA ACC TTC GTG CTG-3'
ITGB6	Fw 5'- GCA AGC TGC TGT GTG TAA GGA A-3' Rv 5'- CTT GGG TTA CAG CGA AGA TCA A-3'
AQP1	Fw 5'- GCC ATC GGC CTC TCT GTA GCC-3' Rv 5'- CTA TTT GGG CTT CAT CTC CAC-3'
KRT24	Fw 5'- CGT CAT CAC CTC TCC TAT TC-3' Rv 5'- AGA CCA CAT CTG CTT CCA-3'
CDH1	Fw 5'- TCT TCA ATC CCA CCA CGT ACA-3' Rv 5'- TGC CAT CGT TGT TCA CTG GA-3'
CLDN6	Fw 5'- TGT TCG GCT TGC TGG TCT AC-3' Rv 5'- CGG GGA TTA GCG TCA GGA C-3'
SNAI2	Fw 5'-CGA ACT GGA CAC ACA TAC AGT G-3' Rv 5'-CTG AGG ATC TCT GGT TGT GGT-3'
BRACHYURY	Fw 5'- TGC TGC AAT CCC ATG ACA-3' Rv 5'- CGT TGC TCA CAG ACC ACA-3'
KRT17	Fw 5'-AAG ATC CGT GAC TGG TAC CAG AGG-3' Rv 5'-GAT GTC GGC CTC CAC ACT CAG G-3'
POSTN	Fw 5'- GAA AGG GAG TAA GCA AGG GAG-3' Rv 5'- ATA ATG TCC AGT CTC CAG GTT G-3'
GAPDH	Fw 5'-GTG GAC CTG ACC TGC CGT CT-3' Rv 5'-GGA GGA GTG GGT GTC GCT GT-3'

**Additional files that are not embedded into this file include:**

Data files S1 to S4

File S1. Upregulated genes specific to fetal amnion in hPSC-amnion at D10, 15 and 20.

File S2. Upregulated gene set-PPARA activates gene expression in D15 and D20 hPSC-amnion comparing with hPSC.

File S3. The overlapped DEGs in groups of D15 and D20 hPSC-amnion comparing with hPSC.

File S4. Upregulated genes in both mid-gestation amnion (compared to early gestation amnion) and later hPSC-amnion (compared to early hPSC-amnion).